

# Supplemental Information

## Down-/Up-Conversion Emission Enhancement by Li Addition: Improved Crystallization or Local Structure Distortion?

Daniel Avram,<sup>†,‡</sup> Bogdan Cojocaru,<sup>§</sup> Ion Tiseanu,<sup>†</sup> Mihaela Florea<sup>§,¶</sup> and Carmen Tiseanu,<sup>\*,†</sup>

<sup>†</sup>National Institute for Laser, Plasma and Radiation Physics, P.O. Box MG-36, RO 76900,  
Bucharest-Magurele, Romania

<sup>‡</sup>Faculty of Physics University of Bucharest, 405 Atomistilor Street, 077125 Magurele-Ilfov,  
Romania

<sup>§</sup>Faculty of Chemistry, University of Bucharest, 4–12 Regina Elisabeta Boulevard, Bucharest,  
Romania

<sup>¶</sup>National Institute of Materials Physics, 405A Atomistilor Street, 077125 Magurele-Ilfov,  
Romania

\*Electronic mail: [carmen.tiseanu@inflpr.ro](mailto:carmen.tiseanu@inflpr.ro)

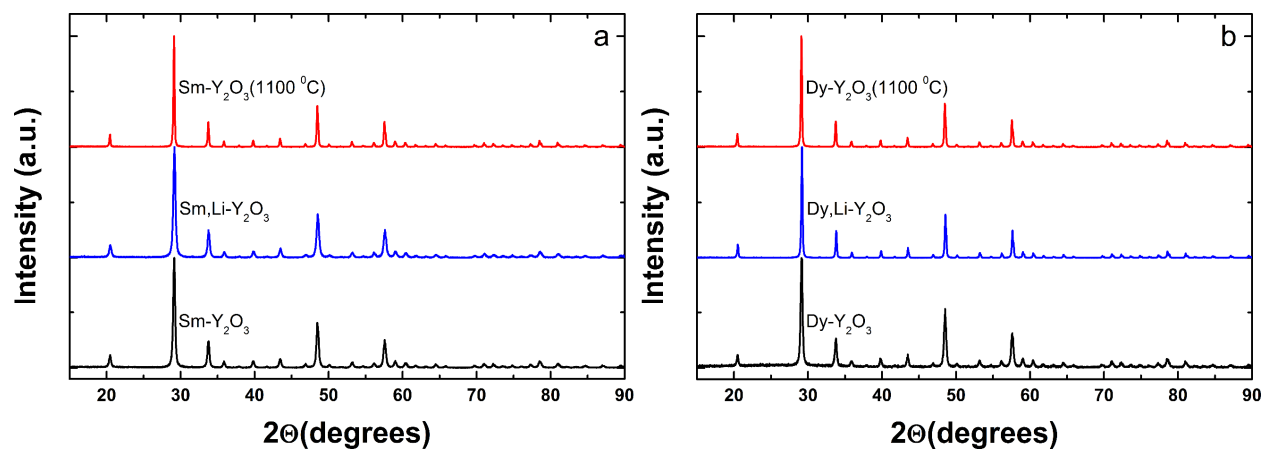


**Figure S1.** The effect of Li addition and calcination temperature on XRD patterns of Sm-Y<sub>2</sub>O<sub>3</sub> and Dy-Y<sub>2</sub>O<sub>3</sub>.

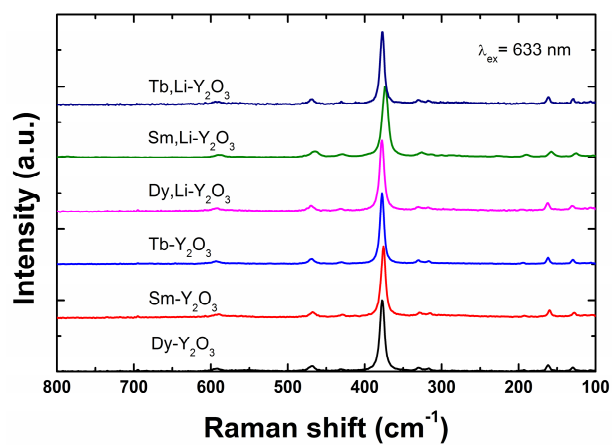


**Figure S2.** The effect of Li addition and calcination temperature on Raman spectra of  $\text{Tb-Y}_2\text{O}_3$ ,  $\text{Sm-Y}_2\text{O}_3$  and  $\text{Dy-Y}_2\text{O}_3$ .

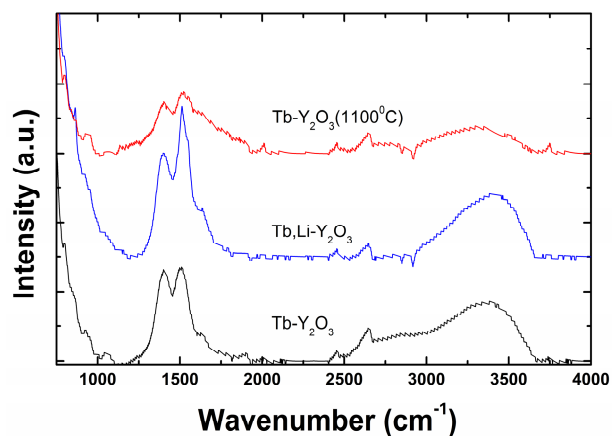


**Figure S3.** The effect of Li addition and calcination temperature on FTIR spectra of Tb-Y<sub>2</sub>O<sub>3</sub>.

The wide band around 3360 cm<sup>-1</sup> are due to OH stretching in the physisorbed water molecules that are roughly similar for Tb- Y<sub>2</sub>O<sub>3</sub> and Tb, Li- Y<sub>2</sub>O<sub>3</sub>. The bands at 1350 and 1510 cm<sup>-1</sup> could correspond to NO<sub>3</sub><sup>-</sup> and CO<sub>3</sub><sup>2-</sup> (hydroxycarbonate like) species absorbed from the preparation procedure. The annealing at 1100°C suppressed significantly the presence of physisorbed water molecules as well as the NO<sub>3</sub><sup>-</sup> and CO<sub>3</sub><sup>2-</sup> species. The effect of Li addition on the intensity of OH band remained inconclusive.

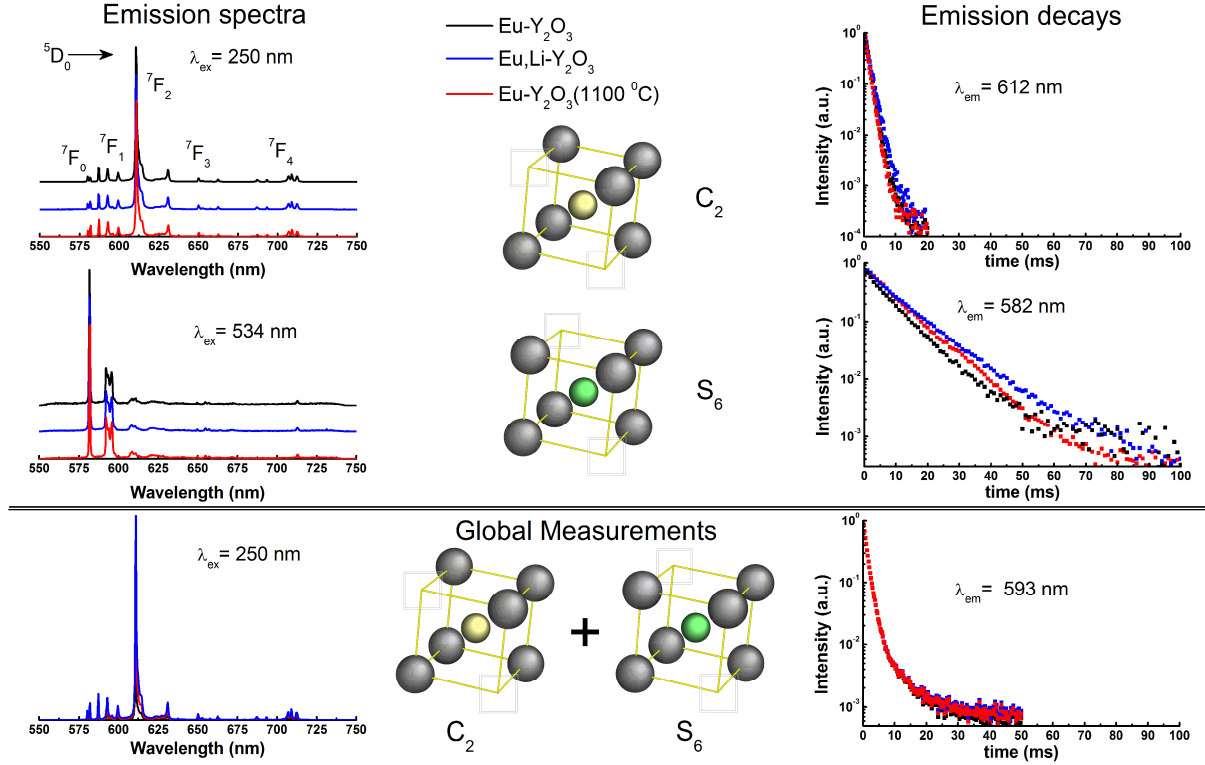


**Figure S4.** Effects of Li addition and increase of the calcination temperature from 800 to 1100 °C on the emission spectra and decays of  $C_2$  and  $S_6$  Eu centers as well as the global measurements. All the emission spectra were normalized to maximum peak intensity. The excitation and emission wavelengths ensured the best spectral separation of the distinct Eu centers. The schematic representations of  $C_2$  and  $S_6$  sites in cubic  $Y_2O_3$  is also illustrated.

The characteristic emissions of  $C_2$  and  $S_6$  Eu centers were obtained by excitation into  $Eu^{3+} - O^{2-}$  charge transfer band and f-f absorption of Eu around 534 nm (corresponding to  ${}^7F_0 - {}^5D_1$  transition), respectively. The  $C_2$  type emission of  $Eu-Y_2O_3$  is dominated by ED (electric dipole)  ${}^5D_0 - {}^7F_2$  transition around 612 nm.<sup>1,2</sup> Conversely, the  $S_6$  type emission of  $Eu-Y_2O_3$  is dominated by the MD (magnetic dipole)  ${}^5D_0 - {}^7F_1$  transition peaked around 585 nm.<sup>1</sup> The average emission lifetime of  $S_6$  Eu is estimated to be around  $\sim 7$  ms, which is five times greater than the value of  $C_2$  Eu ( $\sim 1.4$  ms). Slightly different decays measured for  $S_6$  Eu in the three samples are likely related to incomplete spectral separation of  $S_6$  and  $C_2$  centers.

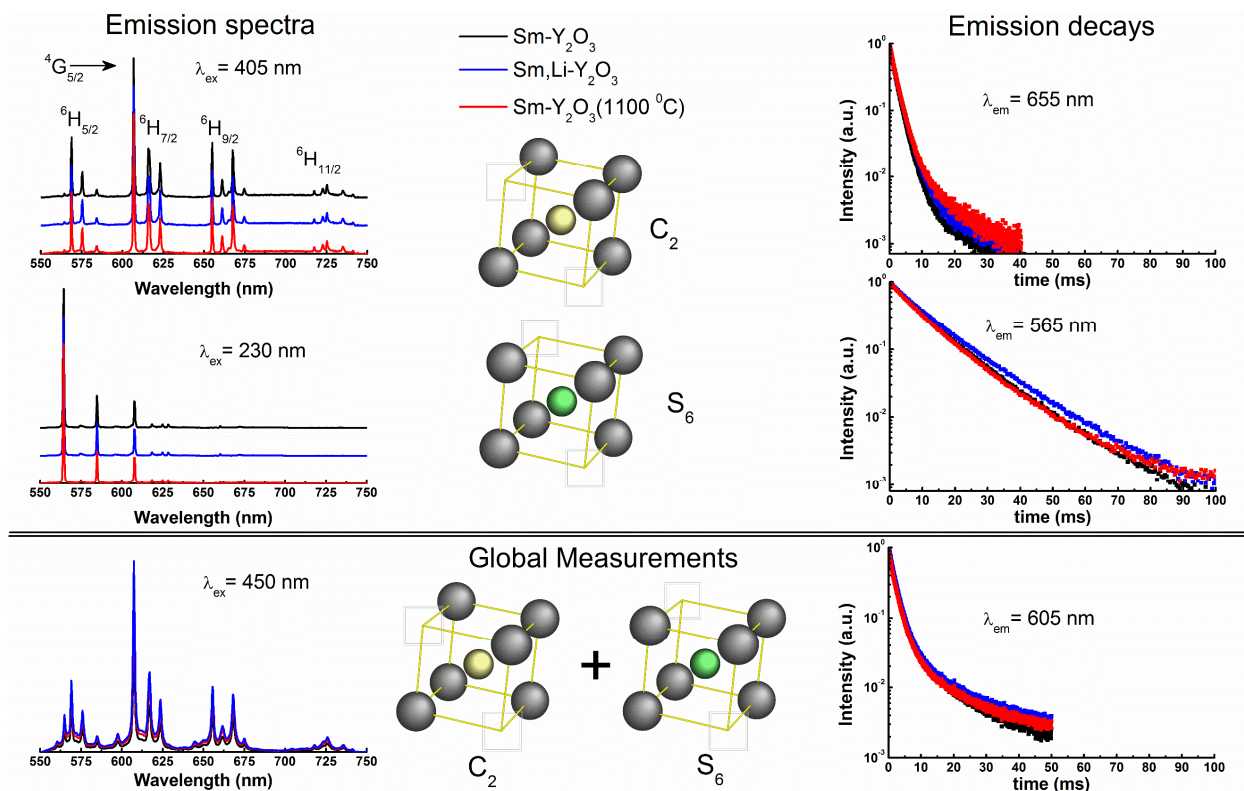


**Figure S5.** Effects of Li addition and increase of the calcination temperature from 800 to 1100 °C on the emission spectra and decays of  $C_2$  and  $S_6$  Sm centers as well as the global measurements. All the emission spectra were normalized to maximum peak intensity. The excitation and emission wavelengths ensured the best spectral separation of the distinct Sm centers. The schematic representations of  $C_2$  and  $S_6$  sites in cubic  $Y_2O_3$  is also illustrated.

The characteristic emissions of  $C_2$  and  $S_6$  Sm centers were obtained by excitation into  $Sm^{3+} - O^{2-}$  charge transfer band and f-f absorption of Sm at 230 and 405 nm, respectively.<sup>3</sup> The  $C_2$  type emission of  $Sm-Y_2O_3$  is dominated by mixed MD (magnetic dipole) + ED (electric dipole)  $^4G_{5/2} - ^6H_{7/2}$  (~608 nm) followed by the MD  $^4G_{5/2} - ^6H_{5/2}$  (~569 nm) and ED  $^4G_{5/2} - ^6H_{9/2}$  (~655 nm) emission transitions. Conversely, the  $S_6$  type emission of  $Sm-Y_2O_3$  is dominated by the MD  $^4G_{5/2} - ^6H_{5/2}$  transition (~565 nm) followed by mixed MD + ED  $^4G_{5/2} - ^6H_{7/2}$  (~608 nm) transition.<sup>3,4</sup> The average emission lifetime of  $S_6$  Sm is estimated to be around ~10 ms, which is roughly 6 times greater than the value of  $C_2$  Sm (~1.8 ms).

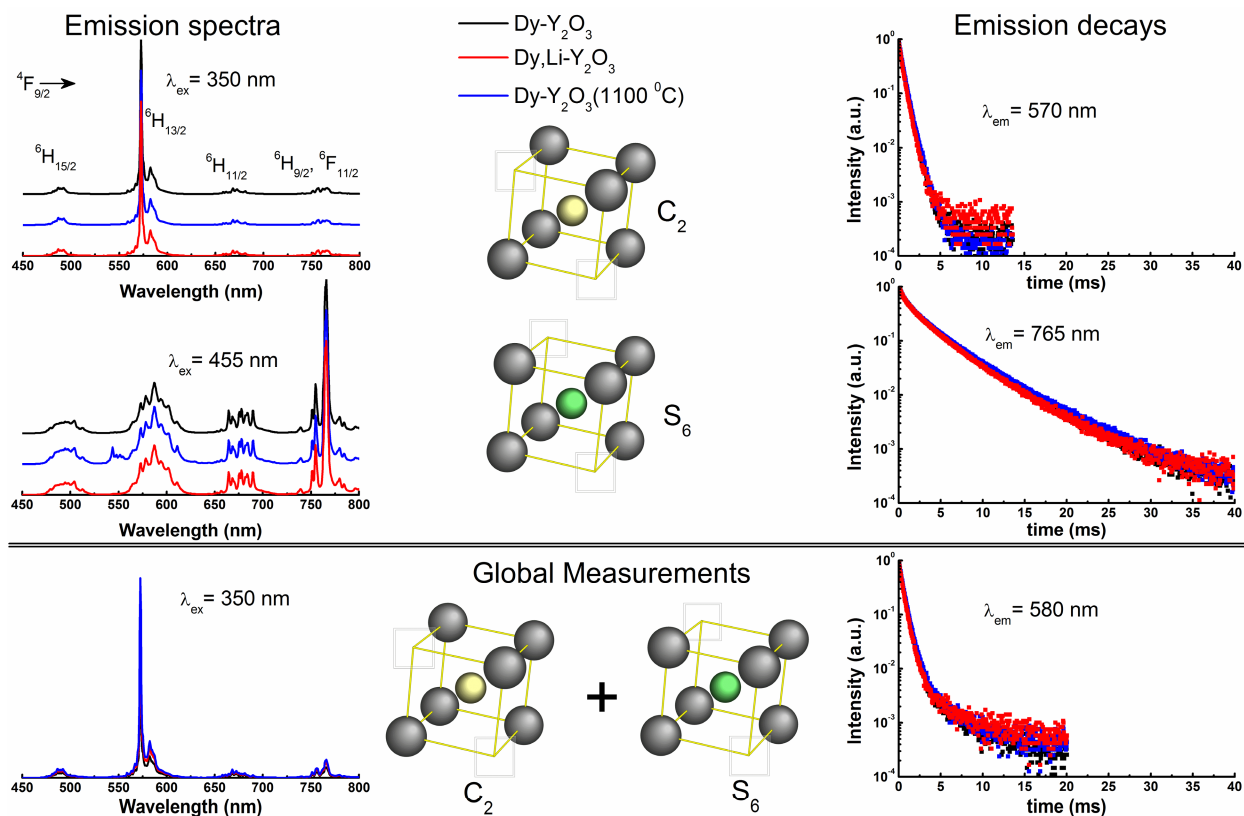


**Figure S6.** Effects of Li addition and increase of the calcination temperature from 800 to 1100 °C on the emission spectra and decays of  $C_2$  and  $S_6$  Sm centers as well as the global measurements. All the emission spectra were normalized to maximum peak intensity. The excitation and emission wavelengths ensured the best spectral separation of the distinct Sm centers. The schematic representations of  $C_2$  and  $S_6$  sites in cubic  $Y_2O_3$  is also illustrated.

The characteristic emissions of  $C_2$  and  $S_6$  Dy centers were obtained by excitation into f-f absorptions of Dy at 350 and 455 nm, respectively.<sup>5</sup> The emission of  $C_2$  Dy is dominated by the  $^4F_{9/2} - ^6H_{13/2}$  yellow transition at 570 nm. The fingerprint emission of  $S_6$  Dy is striking different to that of  $C_2$  Dy with a relatively intense NIR emission corresponding to the MD  $^4F_{9/2} - ^6H_{9/2}/^6F_{11/2}$  transitions around 765 nm.<sup>4</sup> The average emission lifetime of  $S_6$  Dy is estimated to be around 4.8 ms, which is one order of magnitude greater than the value of  $C_2$  Dy (0.43 ms).

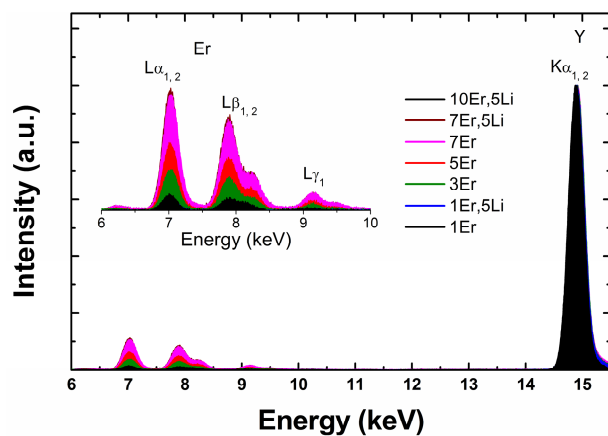


**Figure S7.** Elemental analysis of Er-  $Y_2O_3$  by use of X-ray induced fluorescence. The energy of Er and Y X-ray emission lines were attributed from [http://xdb.lbl.gov/Section1/Table\\_1-2.pdf](http://xdb.lbl.gov/Section1/Table_1-2.pdf)<sup>5</sup>.



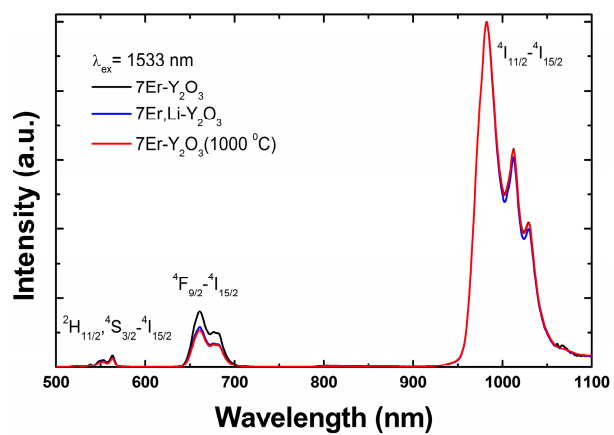


**Figure S8.** Effect of Li addition and extended calcination temperature on the UPC emission shapes of 7Er-Y<sub>2</sub>O<sub>3</sub> under 1533 nm excitation. All spectra were normalized to 980 nm based peak.

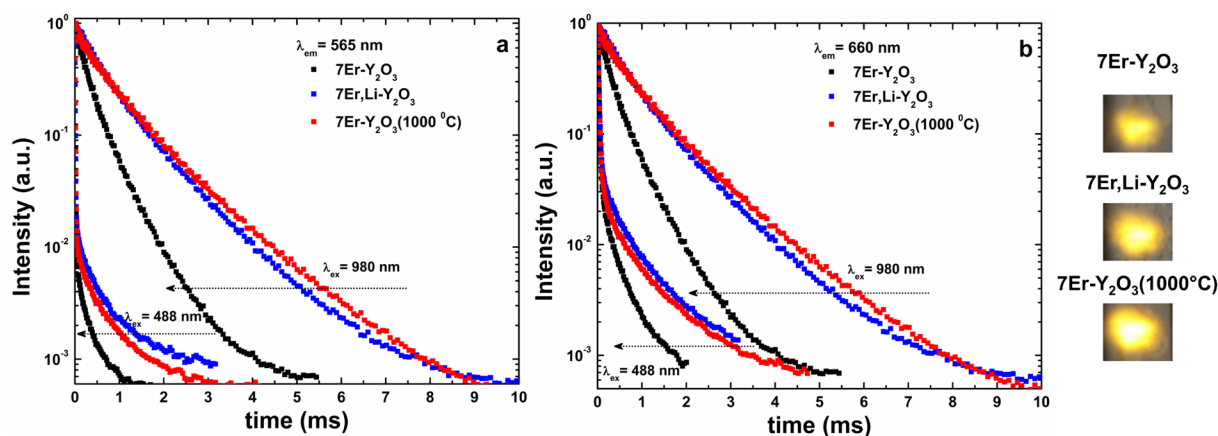


**Figure S9.** Effect of Li addition and extended calcination temperature on the UPC emission decays of 7Er-Y<sub>2</sub>O<sub>3</sub> under excitation at 980 nm. The digital images of the nanopowders were obtained in the *ambient room light conditions* by use of Canon EOS 60D under exposure time of 1s with 400 ISO.

## References:

1. Buijs, M.; Meyerink, A.; Blasse, G.; Energy transfer between Eu<sup>3+</sup> ions in a lattice with two different crystallographic sites: Y<sub>2</sub>O<sub>3</sub>: Eu<sup>3+</sup>, Gd<sub>2</sub>O<sub>3</sub>: Eu<sup>3+</sup> and Eu<sub>2</sub>O<sub>3</sub>. *Journal of luminescence*, **2013**, 37(1), 9-20.
2. Tanner, P.A.; Wong, K.L., Synthesis and spectroscopy of lanthanide ion-doped Y<sub>2</sub>O<sub>3</sub>. *The Journal of Physical Chemistry B*, **2004**, 108(1), 136-142.
3. Lupei, A.; Tiseanu, C.; Gheorghe, C.; Voicu, F.; Optical spectroscopy of Sm<sup>3+</sup> in C<sub>2</sub> and C<sub>3i</sub> sites of Y<sub>2</sub>O<sub>3</sub> ceramics. *Applied Physics B*, **2012**, 108(4), 909-918.
4. Avram, D.; Cojocaru, B.; Florea, M.; Tiseanu, C.; Advances in luminescence of lanthanide doped Y<sub>2</sub>O<sub>3</sub>: case of S<sub>6</sub> sites. *Optical Materials Express*, **2016**, 6(5), 1635-1643.
5. Thompson, A.; Attwood, D.T.; Gullikson, E.; Howells, M.; Kortright, J.; Robinson, A.; X-ray data booklet (2009). URL <http://xdb.lbl.gov>.